

Role of Surface Energy in the Vapor–Liquid–Solid Growth of Silicon

V. A. Nebol'sin and A. A. Shchetinin

Voronezh State Technical University, Moskovskii pr. 14, Voronezh, 394026 Russia

Received December 3, 2002

Abstract—The conditions of vapor-phase Si whisker growth are examined, and the role of the surface Gibbs energy in the vapor–liquid–solid process is evaluated. The mechanism responsible for the catalytic activity of the liquid phase on the tip of Si whiskers is elucidated. Experimental surface tension data are used to estimate the driving force acting on the three-phase line of contact upon a displacement of the liquid droplet in the course of whisker growth.

INTRODUCTION

The unique properties of silicon whiskers are due to the vapor–liquid–solid (VLS) growth mechanism—the only mechanism involving more than two phases in equilibrium with one another [1].

According to the existing concepts [2], a key feature of the VLS mechanism is the catalytic activity of the liquid phase, that is, the large accommodation coefficient of atoms adsorbed on the melt surface and the reduced activation energy for nucleation at the crystal–melt interface. Unfortunately, the processes underlying this “physical catalysis” are not yet fully understood.

The mechanisms of Si whisker growth and shaping were considered in [3, 4] from the viewpoint of the thermodynamic equilibrium of a liquid droplet on the tip of the growing whisker, which can be characterized by the growth angle. This approach made it possible to account for many effects, such as the variation in the whisker radius during unsteady-state growth, the formation of a whisker pedestal, and the stability of cylindrical crystal growth. At the same time, a number of effects could not be understood in the framework of this approach. A question of major importance is the origin of unstable whisker growth.

The objective of this work was to gain detailed insight into the role of interfacial energy in the filamentary growth of silicon in VLS systems.

EXPERIMENTAL

Silicon whiskers were grown on {111} single-crystal substrates in a standard chloride–hydrogen system as described in [2], using gold, copper, and other metal particles as growth leaders. To examine the morphology of etch pits and determine the position of the solid–liquid interface at different stages of whisker growth, we used polished axial sections of the whiskers and substrates. The axial growth rate was determined by the “time marker” method [2]. During changes in tempera-

ture, no nutrient was fed to the reaction zone, so that whisker growth was stopped. The process was restarted only after the temperature was fully stabilized at a new level.

RESULTS AND DISCUSSION

When the substrate is heated to 1300 K and the nutrient gas mixture is fed to the reactor, the solid–liquid interface beneath the Si–metal melt droplet becomes the growth front, the volume of the etch pit decreases, the liquid droplet rises above the substrate surface, its shape changes, and the wetting perimeter decreases. These processes are associated with the formation of interfacial regions parallel to the {111} substrate surface and roof-shaped protrusions at the wetting perimeter, which rapidly merge into a continuous flat front [5]. This leads to melt entrapment in the growing crystal. The rise of the droplet over the substrate surface is accompanied by a reduction in the area of the liquid–solid interface. As a result, the diameter of the growing crystal decreases, and the crystal takes a conical shape. The resulting monohedral solidification front is very flat, which can be established by directly examining polished sections of whiskers and is also evidenced by the sharp boundaries of impurity bands resulting from special vapor-phase doping of whiskers [6].

In addition to the flatness of the {111} growth front, which points to the layer-by-layer growth mechanism, the following features of experimental data warrant attention:

1. During cylindrical crystal growth by the VLS mechanism, Si whiskers typically have a circular cross section owing to the circular wetting perimeter. Lateral faceting develops in later stages, by the vapor–solid mechanism [4].
2. It follows from the morphology of crystals having a circular cross section that the liquid droplet rests on

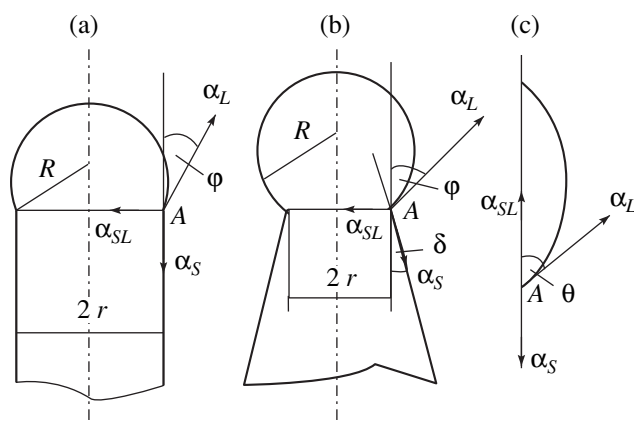


Fig. 1. Geometry of whisker growth: (a) constant radius ($\delta = 0$), (b) decreasing radius ($\delta > 0$), (c) three-phase equilibrium.

the $\{111\}$ growth front, without touching the lateral surface of the whisker.

3. Independent of the growth direction, the flat growth front of silicon whiskers is always parallel to one of the $\{111\}$ singular faces, corresponding to the minimum surface energy.

4. The formation of roof-shaped protrusions always begins at the three-phase line of contact.

5. Kinetic studies [3] give grounds to believe that, at low temperatures, Si whisker growth is a diffusion-limited process, which is in conflict with the layer-by-layer growth of the atomically smooth top face.

6. The observed axial growth rate of whiskers, 1–2 $\mu\text{m/s}$, is almost two orders of magnitude higher than the growth rate of films in an analogous epitaxial process [2].

7. The use of gold, nickel, platinum, and iron as growth leaders ensures steady-state (one-dimensional, oriented) whisker growth, while the process with the participation of silver, zinc, and aluminum is unstable: the liquid droplet breaks down, and the whisker branches and bends. In the presence of tin, bismuth, antimony, and some other elements, no whisker growth occurs.

8. Under steady-state conditions, the crystal diameter often varies, leading to the formation of a conical whisker pedestal.

9. Owing to the oxidation of the Si substrate and the lateral surface of the whisker (in insufficiently pure hydrogen containing oxygen compounds and water vapor), either the droplet does not rise and breaks into smaller droplets or whisker growth is unstable.

10. $\text{Na}_2\text{B}_4\text{O}_7$ applied to the surface of growth leaders residing on an Si substrate leads, at high temperatures in the presence of SiCl_4 , to the formation of through holes in the silicon substrate, which have a diameter typical of whiskers: 1–50 μm .

Consider a liquid droplet on the tip of a whisker. Let the three-phase line of contact adjoin the flat growth front (Fig. 1a). In this configuration, the interfacial tensions α_L (liquid–vapor), α_S (solid–vapor), and α_{SL} (solid–liquid) at point A in the three-phase line cannot be in balance because $\alpha_{SL} < \alpha_L < \alpha_S$ and α_{SL} is normal to α_S . Since the liquid wets only the $\{111\}$ growth front and does not wet the lateral crystal surface, the droplet is in mechanical equilibrium, which can be represented as

$$\alpha_{SL} - \alpha_L \sin \varphi = 0, \quad (1)$$

where φ is the angle between the liquid–vapor interface and the direction of the displacement of the three-phase line (growth angle [7]).

Equation (1) stems from the condition that the vapor–liquid–crystal system is at equilibrium, which means that, at any variations in the droplet shape (without volume changes), the Gibbs energy G of the system remains constant (the minimum possible G at equilibrium, $dG = 0$) [8],

$$G = [\alpha_{SL} \cos^2 \varphi + 2\alpha_L(1 + \sin \varphi)]\pi R^2 = \min, \quad (2)$$

where the first term in square brackets represents the Gibbs energy of the liquid–solid interface, the second term represents the Gibbs energy of the liquid–vapor interface, and R is the droplet radius.

Equating the derivative of Eq. (2) to zero, we obtain Eq. (1), which describes the equilibrium droplet shape, corresponding to the minimum surface Gibbs energy,

$$\frac{\alpha_{SL}}{\alpha_L} = \sqrt{1 - \left(\frac{r}{R}\right)^2}, \quad (3)$$

where r is the whisker radius.

In other words, angle φ corresponds to the minimum surface Gibbs energy of the droplet.

In the absence of external perturbations, the equilibrium shape of the droplet, defined by Eq. (3), remains unchanged in the course of whisker growth, as does the cross section of the growing crystal. For thermodynamic equilibrium to be reached, the shape of the $\{111\}$ growth front must be changed so as to ensure the balance of forces.

In the general case, when the lateral surface of the whisker makes angle δ with the growth axis (conical whisker) (Fig. 1b), Eq. (1) can be rewritten in the form

$$\alpha_S \sin \delta + \alpha_L \sin \varphi = \alpha_{SL}. \quad (4)$$

Let solidification occur through tangential displacement of monatomic steps of height h . Whisker growth is thermodynamically plausible if the total Gibbs energy increment upon a displacement of the droplet by distance h is negative and the three-phase line (point A) shifts in the direction corresponding to the minimum

surface Gibbs energy increment (maximum decrease in total energy), i.e., so that the thermodynamic equilibrium condition is met on the {111} face [7, 9]. The minimum increment of the surface Gibbs energy of a step is

$$\alpha = \alpha_S \sqrt{1 - \left(\frac{\alpha_{SL} - \alpha_L \sin \varphi}{\alpha_S} \right)^2} - \alpha_L \cos \varphi. \quad (5)$$

It includes the reduction in the liquid-vapor interfacial energy ($\alpha_L \cos \varphi$) upon a displacement of the droplet by distance h (monatomic layer thickness) and the solid-vapor interfacial energy increment,

$$\alpha_S \sqrt{1 - [(\alpha_{SL} - \alpha_L \sin \varphi)/\alpha_S]^2}.$$

If

$$\alpha - \alpha_{SL} < 0, \quad (6)$$

steps may form the lateral surface of the whisker at angle δ . In such a case, whisker growth is thermodynamically plausible (the droplet wets the growth front).

The range of angles φ in which whisker growth is thermodynamically plausible can be found by substituting Eq. (4) in

$$\alpha_{SL} + \alpha_L \cos \varphi > \alpha_S \cos \delta. \quad (7)$$

We obtain

$$\frac{\alpha_S}{\alpha_L} < \frac{\sin \varphi + \cos \varphi}{\cos \delta - \sin \delta}. \quad (8)$$

Figure 2 shows the right-hand side of inequality (8) as a function of φ for constant-radius ($\delta = 0$) and conical ($\delta > 0$) whisker growth. The horizontal line shows the ratio $\alpha_S/\alpha_L = 1.33$ for silicon whiskers growing from Au-Si liquid droplets at $\alpha_L = 0.900 \text{ J/m}^2$ and $\alpha_S = 1.200 \text{ J/m}^2$ [2]. In regions I and III (Fig. 2), inequality (8) is not met at small and large φ , and whisker growth by the VLS mechanism is unlikely. Clearly, in regions I and III, the reverse process takes place: silicon etching and vaporization (formation of negative whiskers).

In region II, that is, in a range of angles φ ($\varphi \approx 31^\circ$ to 63° in curve 1 and $\varphi \approx 22^\circ$ to 73° in curve 2, Fig. 2), and also for the above values of α_S and α_L ($\alpha_S/\alpha_L = 1.33$), the droplet shape is such that the energetically favored process is the formation of a new solid-vapor interface, i.e., whisker growth.

Thus, there is a range of contact angles of M-Si melt droplets in which condition (8) is fulfilled and whisker growth is thermodynamically plausible. Beyond this range, whisker growth is impossible.

For $\delta > 0$ (conical whisker growth), the range of contact angles suitable for whisker growth is broader. It is for this reason that one often observes conical whisker growth (pedestal), which is, however, not followed by a cylindrical growth stage. It seems likely that, in such cases, the contact angle falls within the range cor-

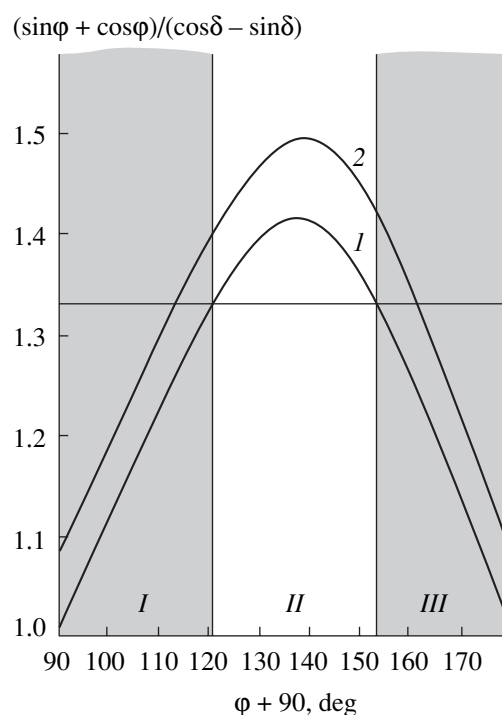


Fig. 2. Plots of $(\sin \varphi + \cos \varphi)/(\cos \delta - \sin \delta)$ against the contact angle of the melt droplet on the whisker tip: (1) constant radius ($\delta = 0$), (2) conical whisker ($\delta > 0$). (I, III) regions of whisker etching and vaporization, respectively, by the SLV mechanism; (II) region of steady-state whisker growth by the VLS mechanism.

responding to whisker growth with $\delta > 0$ but outside the range of growth with $\delta = 0$.

In some M-Si systems, there is a range of angles φ in which the reduction in the total Gibbs energy upon whisker growth is significant; that is, α in Eq. (5) is small and, hence, the difference $\alpha - \alpha_{SL}$ is negative, which ensures stable whisker growth. As is evident from the table, stable growth occurs in the presence of metals with relatively high values of surface energy α_L .

Suitable solvents for Si whisker growth are Au, Ag, Cu (Group I metals), Pt, Pd, and Ni (transition metals), since they have relatively high surface Gibbs energies (table) and α_S/α_L ratios well below 1.41 (Fig. 2, maximum in curve 1, representing constant-radius growth). At the same time, no silicon whiskers can be grown with the participation of Sn, Pb, Sb, Bi, or some other metals for which $\alpha_S/\alpha_L > 1.41$. Whisker growth with the use of Zn, Al, Ga ($\alpha_L = 0.650 \text{ J/m}^2$), or In ($\alpha_L = 0.500 \text{ J/m}^2$) as the solvent yields short, unoriented, tapering crystals, often with globules on their top and other imperfections, which is characteristic of unstable growth.

The development of the {111} growth front is energetically favored because the energy of the Si {111} faces is relatively low. Reducing α_L (e.g., via surfactant adsorption on the melt surface) or increasing α_S (by

Surface Gibbs energy α_L , contact angle $\varphi + 90^\circ$ on $\{111\}$ faces, α_S/α_L ratio, and stability of whisker growth in metal–silicon systems ($\alpha_S = 1.200 \text{ J/m}^2$ [2])

| Metal | $T, \text{ K}$ [8] | $\alpha_L, \text{ J/m}^2$ [8] | α_S/α_L | $\varphi + 90, \text{ deg}$ [10] | Stability of whisker growth |
|-------|--------------------|-------------------------------|---------------------|----------------------------------|-----------------------------|
| Cu | 1400 | 1.300 | 0.97 | 135 | High |
| Au | 1400 | 0.910 | 1.37 | 110 | High |
| Ag | 1300 | 0.900 | 1.33 | – | Intermediate |
| Sn | 1300 | 0.575 | 2.8 | – | No whisker growth |
| Pb | 1300 | 0.400 | 3.15 | – | No whisker growth |
| Pt | 2100 | 1.740 | 0.72 | 120 | High |
| Zn | – | – | – | – | Low |
| Al | 1300 | 0.820 | 1.46 | – | Low |
| Sb | 900 | 0.360 | 3.5 | – | No whisker growth |
| Ni | 1850 | 1.750 | 0.72 | 120 | High |
| Bi | 800 | 0.355 | 3.38 | – | No whisker growth |

removing impurities from the surface layer) may lead to the fulfillment of the condition

$$\alpha_S > \alpha_L \cos \varphi + \alpha_{SL}. \quad (9)$$

The total Gibbs energy increment is then positive, and the reverse process is thermodynamically favored, i.e., silicon vaporization (etching) through the liquid droplet. In other words, if α_L is low compared to α_S , a single (solid–liquid) interface is energetically more favorable than two (solid–vapor and liquid–vapor) interfaces.

Indeed, this process may take place and leads to the formation of either negative whiskers by the solid–liquid–vapor (SLV) mechanism [2] or cylindrical through holes in the silicon substrate, as in the presence of a borax film, which eliminates adsorbed particles and oxides from the silicon surface.

The formation of a thin SiO_2 film on the substrate or lateral whisker surface when the reactant gases are insufficiently pure increases the surface energy α_S and leads to the fulfillment of condition (9). Whisker growth may then become thermodynamically unfavorable, and the process is unstable or does not occur at all.

The energy gain responsible for the accelerated rate of whisker growth in comparison with epitaxial film growth in an analogous chemical process is obviously due to the reduction in the surface Gibbs energy of the liquid phase, α_L , upon the displacement of the three-phase line during whisker growth. For this reason, whisker growth at relatively low temperatures (150–200 K below the Si epitaxy temperature) is diffusion-limited, and the axial growth rate, 1–2 $\mu\text{m/s}$, is notably higher than the rate of epitaxial growth.

The mechanical equilibrium of a liquid droplet, represented by Eq. (1), is due to surface tension forces and results in a circular cross section of the crystal, which reflects the shape of the three-phase line of contact and,

accordingly, the cylindrical shape of the growing whisker. In the course of whisker growth, the three-phase system acts as a natural shaper, determining the diameter and circular cross section of the crystal. Since there is no contact between the crystallizing material and shaper walls, in contrast to many other growth techniques [4, 11], the resulting whiskers have a more perfect structure.

The rise of the liquid droplet during whisker growth (Figs. 1a, 1b) is due to the contact angle hysteresis at the three-phase line. If the contact angle of the lateral whisker surface (φ) is smaller than its equilibrium contact angle (θ) (Fig. 1c), satisfying the Young equation

$$\alpha_L \cos \theta + \alpha_{SL} = \alpha_S, \quad (10)$$

a driving force (F_g) appears, applied to the three-phase line of contact. The magnitude of this force can be found by jointly solving Eq. (10) and inequality (7):

$$F_g = \alpha_L (\cos \varphi - \cos \theta \cos \delta) - \alpha_{SL} (\cos \delta - 1) > 0. \quad (11)$$

At $\delta = 0$, inequality (11) takes the form

$$F_g = \alpha_L (\cos \varphi - \cos \theta) > 0. \quad (12)$$

Condition (12) is fulfilled for $\varphi < \theta$. For this reason, the advance of the droplet along the lateral whisker surface can be thought of as the reverse of liquid spreading over a solid surface, i.e., droplet contraction.

Taking $\theta = 60^\circ$ for the silicon–gold system [3] and using the above values of α_L and α_S , we obtain from Eq. (10) $\alpha_{SL} = 0.750 \text{ J/m}^2$. For constant-diameter whisker growth ($\delta = 0$), we find $\varphi \cong 56.5^\circ$ from Eq. (1) and $\alpha = 0.703 \text{ J/m}^2$ from Eq. (5). Since $\alpha < \alpha_{SL}$, the formation of a new solid–vapor interface is energetically more favorable than the formation of a solid–liquid interface. Finally, from Eq. (12) we obtain the driving

force acting on the droplet during Si whisker growth: $F_g = 0.0467 \text{ J/m}^2$.

CONCLUSIONS

The main effects of interfacial energies on the filamentary growth of silicon in VLS systems are the lowering of the potential barrier to crystallization, owing to the reduction in the surface Gibbs energy of the liquid phase, and the equilibration of the liquid droplet on the whisker tip. The droplet acts as a shaper, being responsible for the circular cross section of the growing crystal.

REFERENCES

1. Maslov, V.N., *Vyrashchivanie profil'nykh poluprovodnikovyykh monokristallov* (Growth of Shaped Semiconductor Crystals), Moscow: Metallurgiya, 1977.
2. Givargizov, E.I., *Rost nitevidnykh i plastinchatykh kristallov iz para* (Vapor Growth of Whiskers and Platelike Crystals), Moscow: Nauka, 1977.
3. Nebol'sin, V.A., Shchetinin, A.A., and Natarova, E.I., Variation in Silicon Whisker Radius during Unsteady-State Growth, *Neorg. Mater.*, 1998, vol. 34, no. 2, pp. 135–137 [*Inorg. Mater.* (Engl. Transl.), vol. 34, no. 2, pp. 87–89].
4. Tatarchenko, V.A., *Ustoichivyy rost kristallov* (Steady-State Crystal Growth), Moscow: Nauka, 1988.
5. Shchetinin, A.A., Kozenkov, O.D., and Nebol'sin, V.A., A Model for the Initial Stages of Silicon Whisker Growth, *Izv. Vyssh. Uchebn. Zaved., Fiz.*, 1989, no. 1, pp. 117–119.
6. Bataronov, I.L., Shchetinin, A.A., Dunaev, A.I., and Korchagin, V.V., Axial Growth Rate of Silicon Whiskers in the Presence of Boron Tribromide, in *Tonkie plenki i nitevidnye kristally* (Thin Films and Whiskers), Voronezh: Voronezh. Pedagogich. Inst., 1993, pp. 92–99.
7. Voronkov, V.V., On the Thermodynamic Equilibrium at a Three-Phase Line of Contact, *Fiz. Tverd. Tela* (Leninograd), 1963, vol. 5, no. 2, pp. 570–574.
8. Naidich, Yu.V., *Kontaktnye yavleniya v metallicheskih rasplavakh* (Contact Phenomena in Metallic Melts), Kiev: Naukova Dumka, 1972.
9. Voronkov, V.V., Processes at the Solidification Interface, *Kristallografiya*, 1974, vol. 19, no. 6, pp. 922–929.
10. Shchetinin, A.A., Bubnov, L.I., Tatarenkov, A.F., and Dolgachev, A.A., *Dinamika izmeneniya kraevykh uglov kapel' na monokristallicheskih podlozhkakh* (Variation in the Contact Angle of Droplets on Single-Crystal Substrates), Available from VINITI, 1987, Moscow, no. 3316-V87.
11. Stepanov, A.V., Growth of Shaped Crystals, *Izv. Akad. Nauk SSSR, Ser. Fiz.*, 1969, vol. 33, no. 12, pp. 1946–1948.

Copyright of Inorganic Materials is the property of Kluwer Academic Publishing / Academic and its content may not be copied or emailed to multiple sites or posted to a listserv without the copyright holder's express written permission. However, users may print, download, or email articles for individual use.